IEEE Access
Multidisciplinary | Rapid Review | Open Access Journal

Received April 9, 2021, accepted April 28, 2021, date of publication May 11, 2021, date of current version May 21, 2021.

Digital Object Identifier 10.1109/ACCESS.2021.3079382

Vanadium Redox Flow Battery State of Charge Estimation Using a Concentration Model and a Sliding Mode Observer

ALEJANDRO CLEMENTE[1], MANUEL MONTIEL[2,3], FÉLIX BARRERAS[3], ANTONIO LOZANO[3], AND RAMON COSTA-CASTELLÓ[1], (Senior Member, IEEE)

[1]Institut de Robòtica i Informàtica Industrial (IRI-CSIC), 08028 Barcelona, Spain
[2]Fundacíon ARAID, Gobierno de Aragón, 50018 Zaragoza, Spain
[3]LIFTEC, CSIC-Universidad de Zaragoza, 50018 Zaragoza, Spain

Corresponding author: Alejandro Clemente (alejandro.clemente.leon@upc.edu)

This work was supported in part by the Spanish National Research Council Consejo Superior de Investigaciones Científicas (CSIC) under Project PIE-201980E101, in part by the Spanish Ministry of Science and Innovation through the Project DOVELAR (Ministerio de Ciencias yUniversidades (MCIU)/Agencia Estatal de Investigación (AEI)/Fondo Europeo de Desarrollo Regional (FEDER), Unión Europea (UE) under Grant RTI2018-096001-B-C31 and Grant RTI2018-096001-B-C32, in part by the Laboratorio de Investigación en Fluidodinámica y Tecnologías de la Combustión (LIFTEC) Research Team through the Aragon Government under Project LMP246_18, and to the group T01_20R, in part by the Universidad Politécnica de Cataluña (UPC) Research Team through the María de Maeztu Seal of Excellence to Instituto de Robótica e Informática (IRI) under Grant MDM-2016-0656, and in part by the Generalitat de Catalunya under Project 2017 SGR482.

ABSTRACT Vanadium redox flow batteries are very promising technologies for large-scale, inter-seasonal energy storage. Tuning models from experimental data and estimating the state of charge is an important challenge for this type of devices. This work proposes a non-linear lumped parameter concentration model to describe the state of charge that differentiates the species concentrations in the different system components and allows to compute the effect of the most relevant over-potentials. Additionally, a scheme, based on the particle swarm global optimization methodology, to tune the model taking into account real experiments is proposed and validated. Finally, a novel state of charge estimation algorithm is proposed and validated. This algorithm uses a simplified version of previous models and a sliding mode control feedback law. All developments are analytically formulated and formally validated. Additionally, they have been experimentally validated in a home-made single vanadium redox flow battery cell. Proposed methods offer a constructive methodology to improve previous results in this field.

INDEX TERMS Vanadium redox flow battery modelling, state of charge estimation, non-linear model tuning from experimental data, particle swarm optimization, sliding mode observer.

I. INTRODUCTION

Redox flow batteries (RFBs) are electrochemical energy storage systems that have certain peculiarities compared to other equivalents such as rechargeable batteries or supercapacitors. This technology has been known since the 19th century, although it was not until the 70s of the last century that NASA and the Exxon company began to investigate these devices. Like a traditional battery, they consist of an anode and a cathode separated by a membrane that isolates the two electrolytes. This membrane prevents the redox species from mixing and facilitates the crossover of ions to maintain the electroneutrality of the system. The main difference from other types of batteries is that the active materials are stored in the form of dissolved electrolytes in reservoirs external to the device. It permits the independent sizing of the device's power (stack size) and its storage capacity (which depends on the nature, volume and concentration of electrolytes). This independence of the power supplied and the energy stored provides greater flexibility both to scale the installations according to the storage time needed, and to update their size based on the energy demand, nature, volume and concentration.

The first RFBs used aqueous solutions of iron and chromium salts as positive and negative electrolyte, respectively. The presence of Fe and Cr ionic species in solutions separated by an ion exchange material was a great problem due to the cross contamination caused by the crossover of ions of different chemical nature through the ion exchanger. In the mid-1980s, the research group of

The associate editor coordinating the review of this manuscript and approving it for publication was Ning Sun.

Prof. Maria Skyllas-Kazacos, from the University of New South Wales, developed a redox system based on vanadium salts in aqueous solution [1]. After various improvements throughout the first decade of the 21st century, the all-vanadium redox flow battery (VRFB) has become the most widely used system and has aroused growing interest among researchers and companies in the energy sector [2]. In contrast to solid-state batteries, VRFBs can provide multiple services, such as peak control, frequency and voltage regulation, or its use as backup systems in electric vehicle fast charging stations. In addition, they present a unique combination of advantages added to the possibility of independent scaling of the energy and power units, such as their high energy efficiency, low environmental impact, tolerance to deep discharges and their long life cycle (>20,000 cycles). Currently, there are numerous studies related to cell design and performance improvements using new components such as electrodes or membranes, but fewer are proposing systems for managing energy in a more efficient way [3], [4].

Unlike other battery types, RFB are active elements and automatic control plays a very important role [5], [6]. Determining the appropriate electrolyte flow [7] and estimating the state of charge are the two main issues from the automatic control point of view. At present, the most widely used methods to estimate the state of charge (SOC) are based on measurements of the open circuit potential (OCP) [8], [9], conductivity [10], viscosity [11] or the colour of the electrolytes [12]. However, these estimates are conditioned by the temperature dependence and the imbalance of electrolytes, so the precision decreases as they are degraded and the battery capacity fades. Moreover, due to their inaccuracy and intrusivity, these techniques are not the best solution for the purpose presented.

State observers [13]–[15] have been efficiently used to estimate relevant variables in dynamic systems; in recent years they have been proposed to determine the VRFB SOC [6]. For SOC monitoring, the most commonly used are the electrochemical models that give a formulation for the chemical species involved in this type of systems. In this scenario, Skyllas-Kazacos proposed a lumped parameter model to monitor the evolution of vanadium species inside the battery [16] based on a non-linear system; other approximations consider an equivalent electrical circuit to simplify the model [17], [18]. The main issue is that their precision depends on the quantity and quality of the measured data, so the predicted SOC can lead to large errors. Other models are based on analysing different variables, such as the pressure, conductivity or temperature of the electrolytes [12]. Although equivalent circuits offer a simple and more intuitive representation, their accuracy is only local (i.e. the circuit parameters might change form one operation point to another).

One of the main difficulties when using electrochemical models, which offer a more global description, is that they cannot be easily tuned from experimental data. This model calibration can be performed online, in real-time, or offline by means of collected data. [5] presents an offline estimation of the standard electrode potential and ohmic resistance parameters. Offline global optimization methods, such as Particle Swarm Optimization (PSO) have already been proposed [19].

Observers combine a given VRFB model, some measurements, system variables and a feedback law to force the convergence between the model and the data. Most VRFB observers are based on the measure of the OCP or temperature, that are easy variables to monitor.

Most popular feedback laws are the Extended Kalman Filter (EKF) and non-linear observers. EKF requires linearising the model around an operation point, consequently it is difficult to guarantee that the observer will work in every operation point. On the contrary, non-linear observers offer a global behaviour with an increase of the mathematical complexity. VRFB pioneer, Prof. Skyllas-Kazacos, developed an EKF observer by means of an electrochemical model and the OCP measure [20]. The same technique was used by means of an equivalent electrical model in [21] or a thermal model with the measure of the electrolyte temperature in [22]. Non-linear observers have also been proposed for VRFB. A Sliding Mode Observer (SMO) is presented in [23] using a dynamic electrical equivalent circuit while a Neural Network (NN) approach is presented in [24] using a multilayer feed-forward network that is trained using the error between open circuit voltage and estimation, with an output layer that computes the SOC. SMOs have the capability to directly deal with non-linear models and handle uncertainty robustly [25].

In order to overcome the limitations of equivalent circuit based observers such as [18], in this work an electrochemical model combined with a SMO is proposed. Although the basic model is taken from the literature [26], it has been improved to take into account the different over-potentials existing in VRFB. Moreover, this concentration model allows cell and tank concentrations to be different, so there is not a direct relationship between the cell voltage and the SOC. Differently from equivalent circuit based observers, the usage of a non-linear model in the observer allows to describe the system behaviour in a global manner without the requirement to be close the equilibrium points [27]. The model is calibrated using experimental data, coming from a home made VRFB, and global optimization methods.

In order to limit the mathematical complexity and the required computational burden required to implement the observer a simplified model is proposed. This simplified model is used to design a SMO which guarantees global performance.

The observer design is based on two steps. Firstly, the simplified system is transformed into a canonical control form, latter a sliding mode controller is included. The variable change which allows to transform the original system into the control canonical form is well-posed, consequently the two spaces are equivalent and the observer can be rewritten in the original coordinates. This methodology formally guarantees sliding mode existence and performance. Reference [13]

Finally, all theoretical developments have been experimentally validated.

The main contributions of this work are the following:

- Improvement of an existing electrochemical model to take into account over-potentials.
- A methodology based on global optimization and experimental data to tune the electrochemical model.
- Formulation of a state of charge estimator based on a simplified nonlinear electrochemical model and sliding mode feedback law.
- Experimental validation of the proposed methodology.

The work is organized as follows: section II describes the proposed VRFB model, section III describes the experimental setup, section IV describes the methodology used to tune the model, section V contains the observer formulation, section VI shows the experimental results and section VII presents the conclusions of the work.

II. VRFB MODEL FORMULATION

This section describes the VRFB model. Firstly, the different concentrations evolution is analyzed. After that, there is a description of how the output voltage and the state of charge (SOC) are computed based on the concentrations.

A. CONCENTRATION EVOLUTION

Skyllas Kazacos [28] introduced a model which allows to describe the evolution of the different concentration vanadium species existing in a VRFB. This model can be written in state-space form as

$$\dot{\boldsymbol{x}} = A\boldsymbol{x} + B_1\boldsymbol{x} \cdot q_1 + B_2\boldsymbol{x} \cdot q_2 + cj \tag{1}$$

where q_1 and q_2 the flow rates of the anolyte and the catholyte parts, j is the VRFB current density and the state vector, $\boldsymbol{x}$, is defined as $\boldsymbol{x}=[c_2^c, c_3^c, c_4^c, c_5^c, c_2^t, c_3^t, c_4^t, c_5^t]^T$; where c_i^k stands for the concentration of vanadium species i in the k, with $k = \{c, t\}$ meaning concentration in the cell and the tank respectively. The sub-index $i = 2$ corresponds to V^{2+}, $i = 3$ to V^{3+}, $i = 4$ to V^{4+} (which exists as VO^{2+}) and $i = 5$ to V^{5+} (which exists as VO_2^+). Matrix $\mathbf{A}$ describes the effect of diffusion, matrices $\mathbf{B}_1, \mathbf{B}_2 \in \mathbb{R}^{8\times8}$ and vector $\mathbf{c} \in \mathbb{R}^8$ describe the effect of the flows and the current over the concentrations respectively. Appendix for Models contains the detailed expression of these elements.

B. STATE OF CHARGE COMPUTATION

The state of charge (SOC) of the VRFB can be understood as the amount of energy stored in the tanks, which can be linked to the amount of V^{2+}, x_5, and V^{5+}, x_8, in the tanks. This amount is usually computed in a per unit manner.

Although in an ideally equilibrated system the SOC would be the same in both reservoirs in practice it might be slightly different in the two tanks (ie. catholyte and anolyte), consequently there are two different ways to compute it

$$SOC_- = \left(\frac{c_2^t}{c_2^t + c_3^t}\right) \tag{2}$$

$$SOC_+ = \left(\frac{c_5^t}{c_4^t + c_5^t}\right). \tag{3}$$

C. CELL VOLTAGE EXPRESSION

The cell voltage (V) is a very important parameter in a VRFB. Jointly with the current it determines the generated/consumed electrical power. Apart from the vanadium concentration in the cell, it depends on the acidity of the medium and several potential loss caused by electrochemical, mass-transfer or charge mobility processes. It can be expressed in terms of the Nerst equation (V^{nerst}), and the existing overpotentials (η).

$$V = V^0 + V^{nerst} + \eta^{act} + \eta^{ohm} \tag{4}$$

where V^0 is the standard electrode potential, η^{act} is the activation overpotential, and η^{ohm} the ohmic overpotential..

The Nerst term can be computed as

$$V^{nerst} = \frac{RT}{nF} \cdot ln\left[\left(\frac{c_5^c \cdot c_{H+}^2}{c_4^c}\right)_{catholyte}\left(\frac{c_2^c}{c_3^c}\right)_{anolyte}\right], \tag{5}$$

where R and F are respectively, the gas and Faraday constants, T is the temperature inside the stack, n the number of electrons involved in the redox reaction (n=1 for VRFB) and c_{H+} is the concentration of protons that can be obtained from the initial concentration ($c_{H+}(0)$) that exists due to the sulphuric acid and the evolution of the V^{5+} concentration:

$$c_{H+} = c_{H+}(0) + c_5^c. \tag{6}$$

The activation overpotential, η^{act}, can be computed from the Butler-Volmer equation considering no mass-transfer effect (electrode surface concentrations do not differ from bulk values) [29]:

$$j_{0,+} = \frac{1}{s_e} \cdot \left(F \cdot k_+^0 \cdot (c_5^c)^{1-\alpha_+} \cdot \left(c_4^c\right)^{\alpha_+}\right) \tag{7}$$

$$j = j_{0,+}\left(e^{\frac{(1-\alpha_+)\cdot n\cdot F}{R\cdot T}\eta_+} - e^{-\frac{\alpha_+\cdot n\cdot F}{R\cdot T}\eta_+}\right) \tag{8}$$

$$j_{0,-} = \frac{1}{s_e} \cdot \left(F \cdot k_-^0 \cdot (c_3^c)^{1-\alpha_-} \cdot \left(c_2^c\right)^{\alpha_-}\right) \tag{9}$$

$$j = j_{0,-}\left(e^{\frac{(1-\alpha_-)\cdot n\cdot F}{R\cdot T}\eta_-} - e^{-\frac{\alpha_-\cdot n\cdot F}{R\cdot T}\eta_-}\right) \tag{10}$$

$$\eta^{act} = \eta_+ - \eta_- \tag{11}$$

where s_e is the electrode surface, j_0 are the exchange current densities at equilibrium, k^θ are the rate constants and α are the change transfer coefficients for the catholyte ($+$) and anolyte ($-$) parts of the system. These relationships define a smooth implicit function $\eta^{act}(j, \boldsymbol{x})$ which provides the activation overpotential.

Finally, the ohmic overpotential can be computed using a constant r that represents the stack resistance:

$$\eta^{ohm} = r \cdot j \cdot s_e$$

III. EXPERIMENTAL PLATFORM

At LIFTEC research facilities a homemade single-cell VRFB with an active area of 3 cm × 3 cm was assembled sandwiching a Nafion 212 membrane between two electrodes of

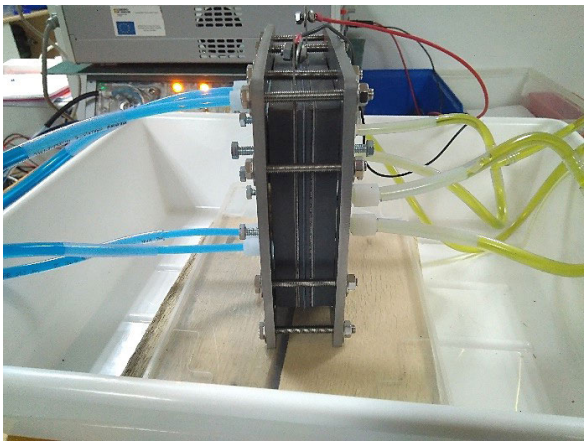

FIGURE 1. Single-cell VRFB designed and built at LIFTEC used in the experiments.

GFD4.6 EA felt thermally activated (Sigracell). It consists in two flowframes manufactured in PVC and two plain graphite bipolar plates. The nafion membrane was pretreated in H_2 O_2 3% for 1 h, and in 0.5 M H_2SO_4 for 1 h, followed by rinsing with water after each step. Electrodes were placed in the PVC flow frames using a symmetric configuration and compressed up to 3 mm (35%). Viton gaskets were used to avoid electrolyte leakage. To close the VRFB, stainless steel end-plates were employed. The single-cell was connected to two reservoirs containing 100 ml of negolyte and posolyte each.

To establish the suitable flow rate for each electrolyte, a 2-channel peristaltic pump (Dinko D-25V2i) was used. The negative reservoir was continuously purged with nitrogen during the experiments to avoid the oxidation of the active species by the atmospheric oxygen. The assembled single-cell can be observed in Fig. 1.

Negolyte and posolyte were prepared from 0.4 M $VOSO_4$, 2.0 M H_2SO_4 and 0.05 M H_3PO_4 solutions by electrolysis in the single-cell in two steps. In the first step, two equal volumes of V^{4+} solutions are transformed in V^{3+} (negolyte) and V^{5+} (posolyte) by charging the cell at a constant voltage of 1.6 V until the current density dropped down to 5 mA $\cdot$ cm^{-2}. In the second one, 100 ml of the generated V^{3+} solution are mixed with the same volume of V^{4+} initial solution. Following the same procedure described in the first step, two equal volumes of $V^{3.5+}$ solution are subjected to electrolysis at 1.6 V until the colour of the solutions has changed to purple (negolyte) and yellow (posolyte).

Charge/discharge cycling was carried out at room temperature with current densities between 100 and 200 mA $\cdot$ cm^{-2}. Negolyte reservoir contained the 100 ml of 0.4 M V^{2+} + V^{3+} while posolyte reservoir contained the 100 ml of 0.4 M V^{4+} + V^{5+} solution. During this procedure, the flow rate for each electrolyte was set to 50 ml $\cdot$ min^{-1}. The upper and lower cell potential cutoff limits were set to 2.0 V and 0.6 V, respectively. Electrolyte generation and charge/discharge experiments were performed using

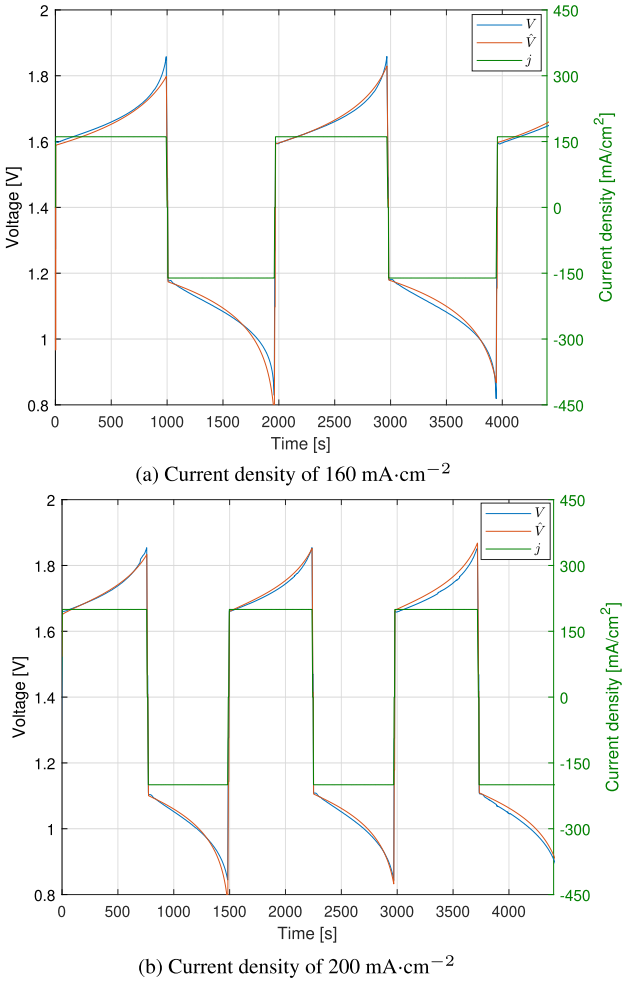

(a) Current density of 160 mA·cm^{-2}

(b) Current density of 200 mA·cm^{-2}

FIGURE 2. Comparison between real and estimated voltages using the calibrated model.

a Metrohm Autolab PGSTAT302 Potentiostat/Galvanostat, which allowed to monitor the current and voltage with a sampling period of 1 second ($T_s = 1$s).

Two charging and discharging processes have been carried out seeking to reach the energy limits of the system, going from a level of total discharge (SOC $\approx$ 0) to that of total charge (SOC $\approx$ 1). Fig. 2 shows the evolution of the measured voltage along these experiments.

IV. MODEL CALIBRATION

Although all parameters of the model described in section II have a clear physical meaning, in practice the uncertainty is important. Additionally, the model neglects many phenomena such as the distributed nature of the VRFB. Due to this a data-based parameter tuning has been performed. To achieve this, the experiments performed in reality are reproduced with the model. To compare the results, the voltage variable, which can be easily measured has been used. Repeating this procedure several times with a different set of parameters the best values for the parameters can be obtained. In other words, an offline optimization problem has been formulated

TABLE 1. System parameters.

Symbol	Meaning	Value
v_c	Cell volume	$1 \cdot 10^{-9}$ m^3
v_t	Tanks volume	$6 \cdot 10^{-5}$ m^3
c_v	Total vanadium concentration	0.4 M
k_2	Diffusion rate of V^{2+}	$6.9 \cdot 10^{-9}$ m$\cdot s^{-1}$ [30]
k_3	Diffusion rate of V^{3+}	$2.5 \cdot 10^{-9}$ m$\cdot s^{-1}$ [30]
k_4	Diffusion rate of V^{4+}	$5.37 \cdot 10^{-9}$ m$\cdot s^{-1}$ [30]
k_5	Diffusion rate of V^{5+}	$4.64 \cdot 10^{-9}$ m$\cdot s^{-1}$ [30]
d	Membrane thickness	0.5 mm
s	Membrane surface area	9 cm^2
s_e	Electrode surface area	9 cm^2
q	Flow rate	100 ml$\cdot$min^{-1}
V^θ	Standard electrode potential	1.27 V

TABLE 2. Parameters bounds.

Parameter	Lower bound	Upper bound
$c_{H+}(0)$	0	4
r	0.1	1.0
α_+	0	1.0
α_-	0	1.0
k_+^θ	10^{-9}	10^{-5}
k_-^θ	10^{-9}	10^{-5}

as follows:

$$\begin{aligned}
&\min_{\mathbf{p}} \sum_{j=1}^{N_{exp}} \frac{1}{n_j} \sum_{l=1}^{n_j} |V(l \cdot T_s) - \hat{V}(l \cdot T_s)| \\
&\text{subject to } \dot{\hat{\mathbf{x}}}(l \cdot Ts) = A\hat{\mathbf{x}}(l \cdot Ts) + B_1\hat{\mathbf{x}} \cdot q_1(l \cdot Ts) \\
&\qquad + B_2\hat{\mathbf{x}} \cdot q_2(l \cdot Ts) + c \cdot j(l \cdot Ts) \\
&\qquad \hat{V}(l \cdot T_s) = h\left(\hat{\mathbf{x}}(l \cdot Ts), j(l \cdot Ts)\right) \\
&\qquad \mathbf{f}(\mathbf{p}) \leq \mathbf{0}.
\end{aligned}$$

where, N_{exp} is the number of available independent experiments (in this work $N_{exp} = 2$), n_j is the length of each experiment, V is measured voltage while $\hat{V}$ is the voltage obtained from the simulation, $\mathbf{p}$ is a vector containing all the variables which are going to be tuned, and $\mathbf{f}$ is a set of constrains that the parameters need to fulfill.

In this work, the tuned variables are the initial proton concentration $c_{H+}(0)$, the ohmic resistance r, and the activation over-potential coefficients α_+, α_-, k_+^θ and k_-^θ. The rest of the parameters are selected directly from the material characteristics and prototype geometry (see TABLE 1).

$\mathbf{f}$ has been used to define the bounds over the achievable values for the tuned variable (see TABLE 2). These bounds have been defined taking into account the literature [5], [29]. The model, the cost function, and some of the constraints contain non-linearities, such as exponentials. This implies that the optimization problem may be non-convex and therefore the use of traditional optimization mechanisms such as the descent by minimum gradient can lead to solutions that correspond to local minima. In order to avoid this problem, global optimization methods are used. In particular, the Particle Swarm Optimization (PSO) method [19] is used because its efficiency in similar problems has been proven. To improve precision and computational efficiency, the PSO is combined with a gradient descent mechanism. This allows to quickly obtain the minimum once the specific attraction basin is entered. [31]. TABLE 3 shows the value of the tuned parameters. Fig. 2 shows both the measured and the simulated voltage values. As it can be seen, although perfect fitting is not achieved, the discrepancies between the model and measurements are small.

TABLE 3. Tuned model parameters.

Parameter	Value
$c_{H+}(0)$	2.32 M
r	0.1413 Ω
α_+	0.5289
α_-	0.5159
k_+^θ	$7.853 \cdot 10^{-6}$ m$\cdot s^{-1}$
k_-^θ	$3.456 \cdot 10^{-6}$ m$\cdot s^{-1}$

V. OBSERVER DESIGN

Although the previously obtained model offers a good fitting, it is not convenient to use it directly to estimate the VRFB SOC due to the fact that it is difficult to precisely estimate the initial value for all state variables. This, jointly with measurement noise and the discrepancies between the model and the experimental data would introduce big discrepancies between the estimated value and the real one. To avoid these discrepancies a state observer [13]–[15] will be used. In the following the development of the state observer is presented.

A. MODEL SIMPLIFICATION

Even it would be possible to design an observer for the model introduced in section II, here the model will be simplified through the introduction of some assumptions. This will allow to obtain a simpler algorithm to estimate the VRFB SOC. This simplification will significantly reduce the required computational burden and consequently allow to implement it in low-cost hardware devices.

In order to simplify the model it is assumed that:

1) The two tanks are equilibrated. In other words, it is assumed that $c_5 = c_2$, $c_3 = c_4$. This indirectly implies that the SOC is the same in both tanks.
2) The amount of vanadium is exactly the same in both tanks, In other words, $c_5 = c_v - c_4$, $c_3 = c_v - c_2$.
3) The flow of electrolytes is exactly the same in both sides, i.e. $q_1 = q_2 = q$. This is the usual hypothesis in most control schemes.

These assumptions are natural because they are the ones that the designer takes into account when designing the battery.

Under these assumptions, the model can be reduced to only one species ($V5^+$) as:

$$\dot{\boldsymbol{x}_r} = A_r\boldsymbol{x}_r + qB_r\boldsymbol{x}_r + c_r j + d_r \tag{12}$$

$\boldsymbol{x}_r=[c_5^c, c_5^t]^T$ being the new state vector, and

$$A_r = \frac{2\cdot s}{v_c\cdot d}\begin{pmatrix}-2k_2-k_5+k_3 & 0\\ 0 & 0\end{pmatrix},\quad c_r = \frac{2s_e}{Fv_c}\begin{pmatrix}1\\0\end{pmatrix}$$
$$B_r = \begin{pmatrix}-\frac{2}{v_c} & \frac{2}{v_c}\\ \frac{1}{v_t} & -\frac{1}{v_t}\end{pmatrix},\quad d_r = \frac{2\cdot s}{v_c\cdot d}\begin{pmatrix}-c_v\cdot k_3\\ 0\end{pmatrix}.$$

The voltage equation would be the one introduced in subsection II-C but applying the introduced constraints.

Under these constrains the system equations become:

$$\dot{\boldsymbol{x}_r} = \mathbf{f}(\boldsymbol{x}_r, \mathbf{u}) \tag{13}$$
$$y = h(\boldsymbol{x}_r, \mathbf{u}) \tag{14}$$

where $y = V$ and $\mathbf{u} = [q, j]$.

This model has been devised to operate inside the observer, so any discrepancy between the simplified model and the experimental data will be corrected by the observer control action.

B. CONTROLLABLE CANONICAL FORM TRANSFORMATION

Most popular observer design techniques require that the system can be written in controllable canonical form (CCF) [13], [32]. In this section the system defined in subsection V-A will be written in CCF. To do so, it is assumed that q and j are known/measurable input variables while the voltage, V, will be the output measurable variable.

In the CCF the new state vector, $\boldsymbol{z}$, is defined by the output and its derivate. In our case:

$$z = \begin{bmatrix}y\\ \dot{y}\end{bmatrix} = \begin{bmatrix}V\\ \dot{V}\end{bmatrix} = \begin{bmatrix}h(\boldsymbol{x}_r, \mathbf{u})\\ L_{\mathbf{f}(\boldsymbol{x}_r,u)}h(\boldsymbol{x}_r, \mathbf{u})\end{bmatrix} = \boldsymbol{\phi}(\boldsymbol{x}_r, u).$$

where L represents the Lie derivative (directional derivative). It can be proven that $\boldsymbol{\phi}$ is a diffeomorphism relating the original state-variables with the new ones. The new dynamics variables can be rewritten as:

$$\dot{z} = \begin{bmatrix}\dot{z_1}\\ \dot{z_2}\end{bmatrix} = \begin{bmatrix}z_2\\ L^2_{\mathbf{f}(\boldsymbol{x}_r,u)}h(\boldsymbol{x}_r, \mathbf{u})\end{bmatrix} \tag{15}$$

which can be rewritten as:

$$\dot{z} = \begin{bmatrix}0 & 1\\ 0 & 0\end{bmatrix}\cdot z + \begin{bmatrix}0\\ \bar{h}(z, u, \dot{u})\end{bmatrix} \tag{16}$$

where $\bar{h}(z, u, \dot{u})$ presents the non-linear part of the model. As $\boldsymbol{\phi}$ is a diffeomorphism, dynamics (16) is analytically equivalent to (13)-(14). Consequently, the evolution of $\boldsymbol{x}_r$ can be reconstructed from that of $\boldsymbol{z}$.

C. SLIDING MODE OBSERVER

In this section, following the developments in previous works [13], [32], a SMO for (16) will be introduced. Firstly, a control action is introduced in the system:

$$\dot{\hat{z}} = \begin{bmatrix}0 & 1\\ 0 & 0\end{bmatrix}\cdot \hat{z} + \begin{bmatrix}0\\ \bar{h}(\hat{z}, u, \dot{u})\end{bmatrix} + \begin{bmatrix}0\\ 1\end{bmatrix} v. \tag{17}$$

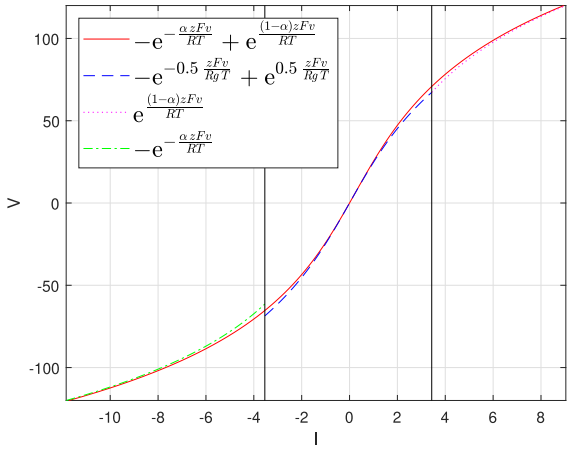

FIGURE 3. Butler-Volmer equation approximation.

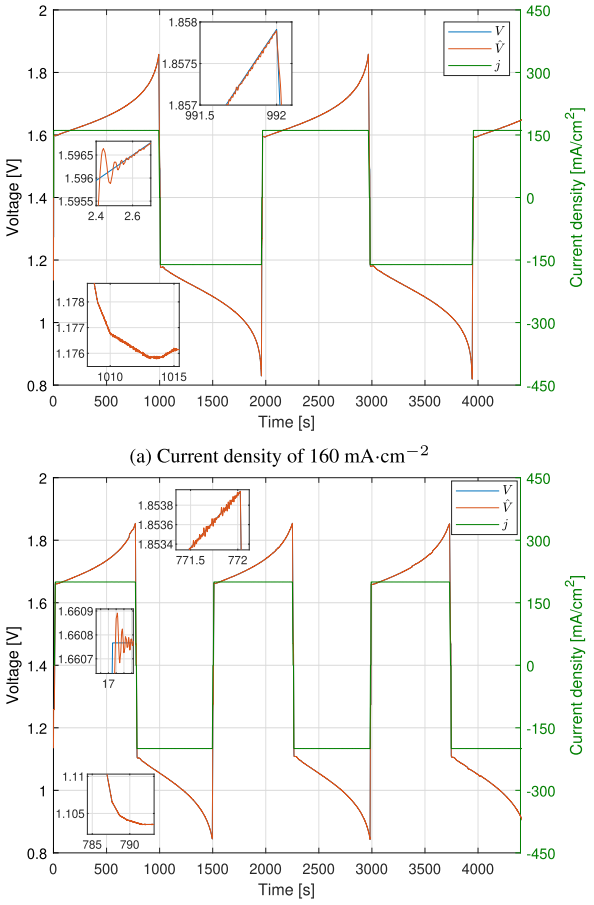

(a) Current density of 160 mA·cm^{-2}

(b) Current density of 200 mA·cm^{-2}

FIGURE 4. Comparison between measured and estimated voltage.

Secondly, to achieve that the voltage estimation, $\hat{z}_1$, converges to the measured voltage, y, the following switching surface, with $e_y = y - \hat{z}_1$, is defined:

$$\sigma = \dot{e}_y + \delta e_y = 0, \tag{18}$$

where $\delta \in \mathbb{R}^+$ is a parameter to be tuned. To achieve this, a second-order quasi-continuous term v is chosen as the

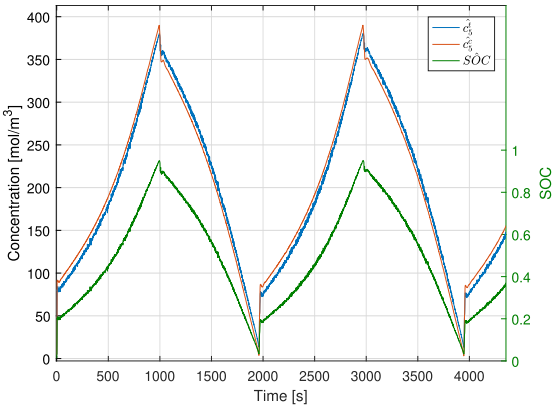

(a) Current density of 160 mA·cm^{-2}

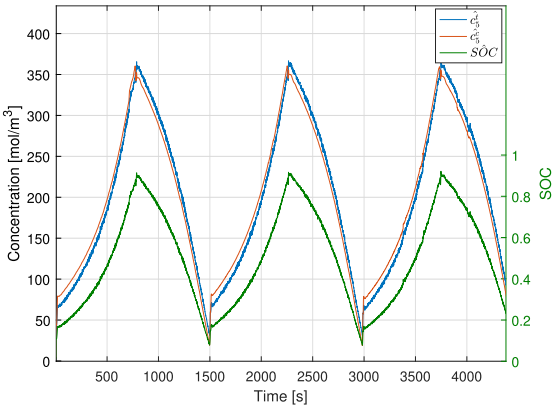

(b) Current density of 200 mA·cm^{-2}

FIGURE 5. Evolution of the SOC and concentrations estimation for the VRFB system.

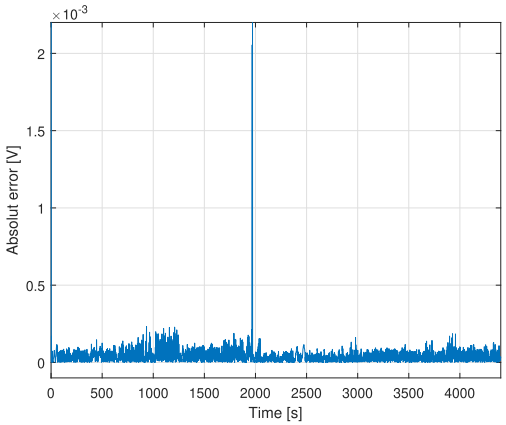

(a) Current density of 160 mA·cm^{-2}

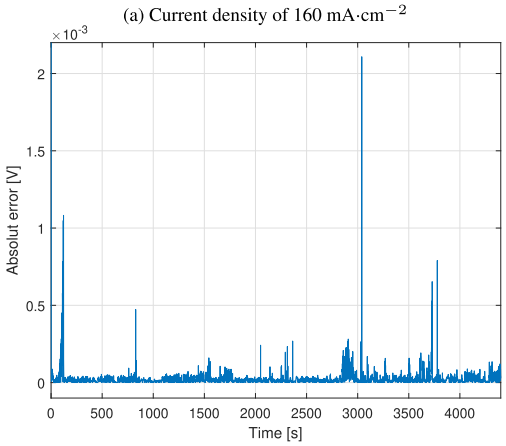

(b) Current density of 200 mA·cm^{-2}

FIGURE 6. Absolute error of estimation.

corrective signal [33]:

$$v = -\gamma \cdot \left(\frac{\dot{\sigma} + |\sigma|^{1/2} \cdot sign(\sigma)}{|\dot{\sigma}| + |\sigma|^{1/2}} \right), \tag{19}$$

γ being the gain of the control action. It must be selected in order to fit the non-linearity term $\bar{h}(z, u, \dot{u})$. As discussed in [13], [32], control law (19), combined with switching surface (18) guarantees that (17) will track the evolution of measured voltage in a stable and robust manner.

Using the diffeomorphism $\boldsymbol{\phi}$, it is possible to write the observer in the original coordinates as:

$$\begin{aligned} \dot{\hat{\boldsymbol{x}}}_r &= A_r \hat{\boldsymbol{x}}_r + qB_r \hat{\boldsymbol{x}}_r + c_r I + d_r + [\boldsymbol{d\phi}]^{-1} v \\ \hat{y} &= h(\hat{\boldsymbol{x}}_r, \mathbf{u}) \end{aligned}$$

where $\boldsymbol{d\phi}$ stands for the jacobian matrix of $\boldsymbol{\phi}$ (i.e $\boldsymbol{d\phi} = \frac{\partial \boldsymbol{\phi}}{\partial \mathbf{x}_r}$).

VI. OBSERVER EXPERIMENTAL VALIDATION

To implement the proposed observer with reduced computational burden, the Butler-Volmer equation is piece-wise approximated as shown in Fig. 3 [34]. This approximation offers small error with a simple implementation.

Additionally to codify (19), it is necessary to compute the first and second derivative of e_y. To do this, a robust differentiator has been used [35].

Although other options are possible, in this work $\delta = 2$, in (18) has been used. This value guarantees a convergence to almost null error in less than 2 s once the sliding regime has been achieved. Finally, $\gamma = 0.8$ has been selected. This value offers a good trade-off between the induced chattering, the observer robustness and the time required to reach the sliding regime.

Fig. 4 presents the evolution of both, the voltage estimation and the measured one in the two experiments, previously discussed in section III. As can be noticed in Fig. 6, for both experiments the absolute error between the real data and the estimated one is almost null, being less than 2 mV. It was also verified that after 25 s the switching surface is almost 0, meaning that the sliding regime has been achieved and that the observer is properly working.

As can be seen, the observer feedback eliminates the discrepancies seen in section III due to uncertain initial conditions and the differences between the model and the real system.

Fig. 5 shows the evolution of the estimated contractions and the computed SOC in the two cases shown in Fig. 4. As it can be seen, there exist small discrepancies between the evolution of the concentration in the cell and the tank, proving that the model differentiates between both concentrations. This difference allows to reproduce the system real

behaviour and obtain a better SOC estimation. Referring to SOC estimation, there are not experimental data to compare with. However, the experiments have been carried out from a minimum to a maximum SOC, and these extremes have been verified by the colours that the electrolytes presented in the tanks. Therefore, the SOC estimation that is displayed for both experiments shows a realistic behaviour.

VII. CONCLUSION

In this work an improved electrochemical model of VRFB has been presented. The used electrochemical model has been improved to take into account the activation overpotentials and other phenomena which usually are not considered in the Literature. Additionally, a methodology to tune the electrochemical model based on experimental data has been proposed.

The model has been shown to be capable of reproducing quite accurately the behaviour of an experimental redox flow battery. Subsequently, a simplified model has been formulated from which a SOC estimator has been proposed. Unlike previous works the designed observer is novel on the use of a nonlinear electrochemical model. This guarantees the global performance and a good approximation in the estimated values in the whole operation range. Regarding the observer, its corrective action allows to obtain an estimation of the SOC with great efficiency, as has been verified experimentally. Moreover, the results have shown the difference that exists between the concentration of species in the cell and the tank, highlighting the need for a model such as the one proposed.

Currently, the authors are working to get a more quantitative validation of the SOC estimation and an online parameters tuning methodology.

APPENDIX
MODELS

The values of matrices A,B_1, B_2 and C appearing in (1) are defined as follows.

$$A = \frac{2 \cdot s}{v_c \cdot d} \begin{pmatrix} -k_2 & 0 & -k_4 & -2k_5 & 0 & 0 & 0 & 0 \\ 0 & -k_3 & 2k_4 & 3k_5 & 0 & 0 & 0 & 0 \\ 3k_2 & 2k_3 & -k_4 & 0 & 0 & 0 & 0 & 0 \\ 2k_2 & -k_3 & 0 & -k_5 & 0 & 0 & 0 & 0 \\ 0 & 0 & 0 & 0 & 0 & 0 & 0 & 0 \\ 0 & 0 & 0 & 0 & 0 & 0 & 0 & 0 \\ 0 & 0 & 0 & 0 & 0 & 0 & 0 & 0 \\ 0 & 0 & 0 & 0 & 0 & 0 & 0 & 0 \end{pmatrix}$$

$$B_1 = \begin{pmatrix} -\frac{2}{v_c} & 0 & 0 & 0 & \frac{2}{v_c} & 0 & 0 & 0 \\ 0 & -\frac{2}{v_c} & 0 & 0 & 0 & \frac{2}{v_c} & 0 & 0 \\ 0 & 0 & 0 & 0 & 0 & 0 & 0 & 0 \\ 0 & 0 & 0 & 0 & 0 & 0 & 0 & 0 \\ \frac{1}{v_t} & 0 & 0 & 0 & -\frac{1}{v_t} & 0 & 0 & 0 \\ 0 & \frac{1}{v_t} & 0 & 0 & 0 & -\frac{1}{v_t} & 0 & 0 \\ 0 & 0 & 0 & 0 & 0 & 0 & 0 & 0 \\ 0 & 0 & 0 & 0 & 0 & 0 & 0 & 0 \end{pmatrix}$$

$$B_2 = \begin{pmatrix} 0 & 0 & 0 & 0 & 0 & 0 & 0 & 0 \\ 0 & 0 & 0 & 0 & 0 & 0 & 0 & 0 \\ 0 & 0 & -\frac{2}{v_c} & 0 & 0 & 0 & \frac{2}{v_c} & 0 \\ 0 & 0 & 0 & -\frac{2}{v_c} & 0 & 0 & 0 & \frac{2}{v_c} \\ 0 & 0 & 0 & 0 & 0 & 0 & 0 & 0 \\ 0 & 0 & 0 & 0 & 0 & 0 & 0 & 0 \\ 0 & 0 & \frac{1}{v_t} & 0 & 0 & 0 & -\frac{1}{v_t} & 0 \\ 0 & 0 & 0 & \frac{1}{v_t} & 0 & 0 & 0 & -\frac{1}{v_t} \end{pmatrix}$$

$$C = \frac{2s_e}{Fv_c}(1, -1, -1, 1, 0, 0, 0, 0)^T$$

ACKNOWLEDGMENT

The authors would like to thanks Alvaro Ibañez during the experimental measurement campaign.

REFERENCES

[1] M. Skyllas-Kazacos, "All-vanadium redox battery," U.S. Patent 4 786 567, Nov. 1988.

[2] M. Skyllas-Kazacos and J. McCann, "Vanadium redox flow batteries (VRBs) for medium- and large-scale energy storage," in *Advances in Batteries for Medium and Large-Scale Energy Storage* (Woodhead Publishing Series in Energy), C. Menictas, M. Skyllas-Kazacos, and T. M. Lim, Eds. Woodhead Publishing, 2015, ch. 10, pp. 329–386, doi: 10.1016/B978-1-78242-013-2.00010-8.

[3] Z. Wei, A. Bhattarai, C. Zou, S. Meng, T. M. Lim, and M. Skyllas-Kazacos, "Real-time monitoring of capacity loss for vanadium redox flow battery," *J. Power Sources*, vol. 390, pp. 261–269, Jun. 2018, doi: 10.1016/j.jpowsour.2018.04.063.

[4] L. F. Arenas, C. P. D. León, and F. C. Walsh, "Engineering aspects of the design, construction and performance of modular redox flow batteries for energy storage," *J. Energy Storage*, vol. 11, pp. 119–153, Jun. 2017, doi: 10.1016/j.est.2017.02.007.

[5] X. Binyu, Z. Jiyun, and L. Jinbin, "Modeling of an all-vanadium redox flow battery and optimization of flow rates," in *Proc. IEEE Power Energy Soc. Gen. Meeting*, Dec. 2013, pp. 1–5, doi: 10.1109/PESMG.2013.6672599.

[6] A. Clemente and R. Costa-Castelló, "Redox flow batteries: A literature review oriented to automatic control," *Energies*, vol. 13, no. 17, p. 4514, Sep. 2020, doi: 10.3390/en13174514.

[7] A. Clemente, G. A. Ramos, and R. Costa-Castelló, "Voltage H_∞ control of a vanadium redox flow battery," *Electronics*, vol. 9, no. 10, p. 1567, 2020.

[8] A. Trovo, "Battery management system for industrial-scale vanadium redox flow batteries: Features and operation," *J. Power Sources*, vol. 465, Jul. 2020, Art. no. 228229, doi: 10.1016/j.jpowsour.2020.228229.

[9] T. Haisch, H. Ji, and C. Weidlich, "Monitoring the state of charge of all-vanadium redox flow batteries to identify crossover of electrolyte," *Electrochimica Acta*, vol. 336, Mar. 2020, Art. no. 135573, doi: 10.1016/j.electacta.2019.135573.

[10] M. Skyllas-Kazacos and S. Corcuera, "State-of-charge monitoring and electrolyte rebalancing methods for the vanadium redox flow battery," *Eur. Chem. Bull.*, vol. 1, no. 12, pp. 511–519, 2012, doi: 10.17628/ecb.2012.1.511-519.

[11] X. Li, J. Xiong, A. Tang, Y. Qin, J. Liu, and C. Yan, "Investigation of the use of electrolyte viscosity for online state-of-charge monitoring design in vanadium redox flow battery," *Appl. Energy*, vol. 211, pp. 1050–1059, Feb. 2018, doi: 10.1016/j.apenergy.2017.12.009.

[12] M. Skyllas-Kazacos and M. Kazacos, "State of charge monitoring methods for vanadium redox flow battery control," *J. Power Sources*, vol. 196, no. 20, pp. 8822–8827, Oct. 2011, doi: 10.1016/j.jpowsour.2011.06.080.

[13] J. Davila, L. Fridman, A. Pisano, and E. Usai, "Finite-time state observation for non-linear uncertain systems via higher-order sliding modes," *Int. J. Control*, vol. 82, no. 8, pp. 1564–1574, Aug. 2009.

[14] A. Cecilia and R. Costa-Castello, "High gain observer with dynamic deadzone to estimate liquid water saturation in PEM fuel cells," *Revista Iberoamericana de Automatica e Informatica Ind.*, vol. 17, no. 2, pp. 169–180, 2020.

[15] A. Cecilia, M. Serra, and R. Costa-Castelló, "Nonlinear adaptive observation of the liquid water saturation in polymer electrolyte membrane fuel cells," *J. Power Sources*, vol. 492, Apr. 2021, Art. no. 229641.
[16] A. Tang, J. McCann, J. Bao, and M. Skyllas-Kazacos, "Investigation of the effect of shunt current on battery efficiency and stack temperature in vanadium redox flow battery," *J. Power Sources*, vol. 242, pp. 349–356, Nov. 2013, doi: 10.1016/j.jpowsour.2013.05.079.
[17] Y. R. Challapuram, G. M. Quintero, S. B. Bayne, A. S. Subburaj, and M. A. Harral, "Electrical equivalent model of vanadium redox flow battery," in *Proc. IEEE Green Technol. Conf. (GreenTech)*, Apr. 2019, pp. 1–4, doi: 10.1109/GreenTech.2019.8767145.
[18] D. Han, K. Yoo, P. Lee, S. Kim, S. Kim, and J. Kim, "Equivalent circuit model considering self-discharge for SOC estimation of vanadium redox flow battery," in *Proc. 21st Int. Conf. Electr. Mach. Syst. (ICEMS)*, Oct. 2018, pp. 2171–2176, doi: 10.23919/ICEMS.2018.8549343.
[19] B. Xiong, Z. Wang, Y. Li, K. Qin, J. Chen, and J. Mu, "An optimal operational strategy for vanadium redox flow battery based on particle swarm optimization," in *Proc. IEEE Innov. Smart Grid Technol.-Asia (ISGT Asia)*, May 2019, pp. 2639–2643.
[20] B. Xiong, J. Zhao, Z. Wei, and M. Skyllas-Kazacos, "Extended Kalman filter method for state of charge estimation of vanadium redox flow battery using thermal-dependent electrical model," *J. Power Sources*, vol. 262, pp. 50–61, Sep. 2014, doi: 10.1016/j.jpowsour.2014.03.110.
[21] M. R. Mohamed, H. Ahmad, M. N. A. Seman, S. Razali, and M. S. Najib, "Electrical circuit model of a vanadium redox flow battery using extended Kalman filter," *J. Power Sources*, vol. 239, pp. 284–293, Oct. 2013, doi: 10.1016/j.jpowsour.2013.03.127.
[22] X. Binyu, J. Zhao, W. Zhongbao, and Z. Chenda, "State of charge estimation of an all-vanadium redox flow battery based on a thermal-dependent model," in *Proc. IEEE PES Asia–Pacific Power Energy Eng. Conf. (APPEEC)*, Dec. 2013, pp. 1–6, doi: 10.1109/APPEEC.2013.6837290.
[23] B. Xiong, H. Zhang, X. Deng, and J. Tang, "State of charge estimation based on sliding mode observer for vanadium redox flow battery," in *Proc. IEEE Power Energy Soc. Gen. Meeting*, Jul. 2017, pp. 1–5, doi: 10.1109/PESGM.2017.8274042.
[24] H. Niu, J. Huang, C. Wang, X. Zhao, Z. Zhang, and W. Wang, "State of charge prediction study of vanadium redox-flow battery with BP neural network," in *Proc. IEEE Int. Conf. Artif. Intell. Comput. Appl. (ICAICA)*, Jun. 2020, pp. 1289–1293.
[25] H. Chen and N. Sun, "Nonlinear control of underactuated systems subject to both actuated and unactuated state constraints with experimental verification," *IEEE Trans. Ind. Electron.*, vol. 67, no. 9, pp. 7702–7714, Sep. 2020.
[26] M. Skyllas-Kazacos and L. Goh, "Modeling of vanadium ion diffusion across the ion exchange membrane in the vanadium redox battery," *J. Membrane Sci.*, vols. 399–400, pp. 43–48, May 2012.
[27] H. Chen and N. Sun, "An output feedback approach for regulation of 5-DOF offshore cranes with ship yaw and roll perturbations," *IEEE Trans. Ind. Electron.*, early access, Feb. 2, 2021, doi: 10.1109/TIE.2021.3055159.
[28] R. Badrinarayanan, J. Zhao, K. J. Tseng, and M. Skyllas-Kazacos, "Extended dynamic model for ion diffusion in all-vanadium redox flow battery including the effects of temperature and bulk electrolyte transfer," *J. Power Sources*, vol. 270, pp. 576–586, Dec. 2014, doi: 10.1016/j.jpowsour.2014.07.128.
[29] S. K. Murthy, A. K. Sharma, C. Choo, and E. Birgersson, "Analysis of concentration overpotential in an all-vanadium redox flow battery," *J. Electrochem. Soc.*, vol. 165, no. 9, pp. A1746–A1752, 2018.
[30] B. Xiong, J. Zhao, Y. Su, Z. Wei, and M. Skyllas-Kazacos, "State of charge estimation of vanadium redox flow battery based on sliding mode observer and dynamic model including capacity fading factor," *IEEE Trans. Sustain. Energy*, vol. 8, no. 4, pp. 1658–1667, Oct. 2017.
[31] M. M. Noel, "A new gradient based particle swarm optimization algorithm for accurate computation of global minimum," *Appl. Soft Comput.*, vol. 12, no. 1, pp. 353–359, Jan. 2012.
[32] J. Luna, R. Costa-Castelló, and S. Strahl, "Chattering free sliding mode observer estimation of liquid water fraction in proton exchange membrane fuel cells," *J. Franklin Inst.*, vol. 357, no. 18, pp. 13816–13833, Dec. 2020.
[33] A. Levant, "Higher-order sliding modes, differentiation and output-feedback control," *Int. J. Control*, vol. 76, nos. 9–10, pp. 924–941, Jan. 2003.
[34] P. Vijay and M. O. Tadé, "Improved approximation for the butler-volmer equation in fuel cell modelling," *Comput. Chem. Eng.*, vol. 102, pp. 2–10, Jul. 2017.
[35] A. Levant, "Robust exact differentiation via sliding mode technique," *Automatica*, vol. 34, no. 3, pp. 379–384, Mar. 1998.

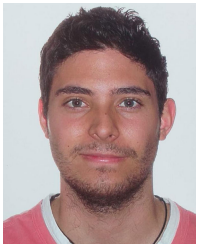

ALEJANDRO CLEMENTE received the B.S. degree in industrial and automatic electronic engineering and the M.S. degree in robotics and automatic control from UPC, in 2018 and 2020, respectively. He is currently a part-time Associate Professor with the Automatic Systems and Industrial Informatics Department, East School of Industrial Engineering, Barcelona. His research interests include the modeling and control of energy management systems, especially is focused on the redox flow batteries.

MANUEL MONTIEL received the B.Sc. and Ph.D. degrees in chemistry from the University of La Rioja, Spain, in 2002 and 2006, respectively. Since 2018, he has been an ARAID Senior Researcher with the Laboratory of Research in Fluid Dynamics and Combustion Technologies (LIFTEC), Zaragoza, Spain. He has authored scientific articles related to chemical synthesis, materials for energy applications, and electrochemistry. His research interests include electrochemical energy storage systems, fuel cells, and electrocatalysis.

FÉLIX BARRERAS received the B.S. and M.S. degrees in mechanical engineering, with the specialization in energy, from the University of Matanzas, Cuba, and the Ph.D. degree in industrial engineering (fluid mechanics) from the University of Zaragoza, Spain. Since 2001, he has been a Senior Researcher with the Laboratory for Research in Fluid dynamics and Combustion Technologies (LIFTEC), a joint center of the Spanish National Research Council (CSIC) and the University of Zaragoza. His areas of expertise are PEM fuel cell design and applications, experimental fluid mechanics, and liquid atomization.

ANTONIO LOZANO received the M.Sc. degree in physics from the University of Zaragoza, Zaragoza, Spain, in 1984, and the Ph.D. degree in mechanical engineering from Stanford University, in 1992. He holds a position of scientific researcher with the Laboratory for Research in Fluid Dynamics and Combustion Technology, a joint center between the Spanish National Research Council and the University of Zaragoza. His areas of expertise are fuel cell design and applications, experimental fluid mechanics. and liquid atomization.

RAMON COSTA-CASTELLÓ (Senior Member, IEEE) was born in Lleida in 1970. He is currently an Associate Professor with the Automatic Control Department, UPC, and the Institut de Robòtica i Informàtica Industrial, a Joint Research Center of the Spanish Council for Scientific Research (CSIC) and UPC. His research interest includes analysis and development of energy management systems (automotive and stationary applications). He is a member of the Comité Español de Automática (CEA) and IFAC (EDCOM, TC 9.4 Committee).